

Earlier detection of brain cells mutation using region based fast convolutional neural networks (RFCNN)

Para Rajesh,

Computer Science and Engineering Dept.,

Gokaraju Rangaraju Institute of

Engineering and Technology

Hyderabad-500090, Telangana, India.

Email: ppr21@gmail.com

A.Punitha,

Computer Science and Engineering Dept.,

Annamalai University,

Annamalai Nagar - 608002,

Tamil Nadu, India.

Email: 12charuka17@gmail.com

P.Chandra Sekhar Reddy,

Computer Science and Engineering Dept.,

Gokaraju Rangaraju Institute of

Engineering and Technology,

Hyderabad-500090, Telangana, India.

Email: pchandureddy@yahoo.com

Received 2022 March 15; **Revised** 2022 April 20; **Accepted** 2022 May 10.

Abstract:

A brain tumor is formed by a group of tissue where anomalous cells are gradually added and the most challenging task is classifying brain tumor using magnetic resonance imaging (MRI) to provide treatment for affected patients. Generally, tumor detection and classification for brain MRI images are investigated by human. Images are interpreted based on the classification for which several approaches are designed. Information about anatomical patterns and abnormal tissues are obtained from segmentation of brain tumor MRI using the proposed RFCNN segmentation technique. Here the dataset of patients with earlier symptoms of brain tumor has been taken along with their pre-historic medical data. Segmentation has been done to predict the presence of brain tumor whether it is mutation of primary tumor cells (non-cancerous) or secondary tumor cells (cancerous). The proposed neural model can analyse MRI images for detecting the cell mutation and pre-processing of input images to eliminate the parts like skull or vertebral column in advance. The efficiency of the method proposed using a MRI image dataset is compared against existing machine learning and deep learning models. From the results, it is observed that this proposed model obtained a remarkable accuracy, AUC, precision, recall and F-1 score for tumor classification than the methods which used the same dataset.

Keywords: brain tumor, MRI tumor, segmentation, RFCNN, classification accuracy

1. Introduction:

In human body, the brain is an enormous and complex organ that controls the whole nervous system, and it contains around 100-billion nerve cells [1]. This essential organ is originated in the center of nervous system. Therefore, any kind of abnormality that exists in the brain may put human health in danger. Among such abnormalities, brain tumors are the most severe ones. Brain tumors are uncontrolled and unnatural growth of cells in the brain that can be classified into two groups such as primary tumors and secondary tumors. The primary tumors present in the brain tissue, while the secondary tumors expand from other parts to the brain tissue through the bloodstream [2]. Among the primary tumors, glioma and meningioma are two lethal types of brain tumors which may lead to death if not diagnosed at the earlier stage [3]. In fact, the most common brain tumor in humans is glioma [4]. As per World Health Organization (WHO), brain tumors are categorized as four grades. The grade 1 and grade 2 tumors describe lower-level tumors (e.g., meningioma), while grade 3 and grade 4 tumors consist of more severe ones (e.g., glioma). In clinical aspects, the rate of incidence for meningioma, pituitary, and glioma tumors are approximately 15%, 15%, and 45%, correspondingly. There are different ways to treat brain tumors based on its size, location, and type. Commonly, surgery is the treatment for brain tumors as it has no side effects on the brain [5]. Various types of medical imaging techniques like computed tomography (CT), magnetic resonance imaging (MRI) and positron emission tomography (PET) are available which are involved in observing the conditions of internal human organs. Among all these imaging modalities, MRI is considered most preferable as it is the only non-invasive and nonionizing modality that offers valuable information in 2D and 3D formats about brain tumor type, size, shape, and position [6]. However, manually reviewing these images are hectic, consumes more time and even there are chances for errors due to the influx of patients [7]. To address this problem, the development of an automatic computer-aided diagnosis (CAD) model is necessary to alleviate the function of classification and diagnosing brain MRI which is

supportive for radiologists and doctors. Several efforts have been made to develop a highly accurate and robust solution for the automatic classification of brain tumors. Nevertheless, due to the variations in inter and intra shape, contrast and texture, classification and diagnosis is still a challenging task. The traditional machine learning (ML) techniques rely on handcrafted features, which restrains the robustness of the solution. Whereas the deep learning-based techniques automatically extract meaningful features which offer significantly better performance. However, deep learning-based models are in need of numerous annotated data for training, and acquiring such data is a challenging task. To obtain a solution for these issues, this study proposes a hybrid solution that exploits (1) region based fast convolutional neural networks (RFCNN) as segmentation to segment powerful and discriminative deep features from brain MRI, and (2) various ML classifiers to identify the normal and abnormal images. Also, to investigate the benefits of combining features from different RFCNN models, we designed the novel segmentation for the MRI-based brain tumor classification task.

The layout of this study is presented as follows: The works related to this research work is discussed in Section 2. The proposed model is presented in Section 3. The experimental setup along with its results are discussed in Section 4. The conclusion is described in Section 5.

2. Related Works:

In the past, development of machine learning approaches helped in discovering the features representing data which is the basis for Deep Neural Networks (DNNs) [8], transforming the problems to solutions from feature-driven into data-driven. Within DNN, in several applications, Convolutional Neural Networks (CNN) [9] and Fully Convolutional Networks (FCN) [10] were applied. Generally, these are extensively employed in image processing [11] and particularly in analysing medical images [12]. Deep Learning has greater impact in designing medical imaging systems and several technologies were widely developed over the past few years [13]. The advancements in this field have motivated machine learning scientists and radiologists. In [14], fully convolutional system was used with BRATS 2013 database, next to kNN classifier [15]. Several recent classification methods of brain tumor using Deep Learning involves CNNs or FCNs. In [16], multi-scale CNN was used for segmenting brain tissues and white matter hyperintensities. Imaged from MRBrainS13 [17] was used in evaluating CNN architecture. In [18], U-net based on CNN was designed for segmenting neural patterns in electron microscopy images. This was named as U as it involved 5 stages of convolutional and de-convolutional each. The aim was in segmenting brain tumor regions with no classification. In [19], new Deep Learning technique was developed for segmentation and classification of tumor. In [20], a deep learning classifier was designed in combination with discrete wavelet transform (DWT) and principal components analysis (PCA) for the classification of a dataset into three classes of brain tumors. In [21], a two-layer CNN architecture was designed for classification of tumors. In [22], CNN method was involved in classification and KELM approach was used as a learning algorithm which took the features extracted by CNN as inputs. This model contains several layers of hidden nodes. In [23], a CNN network with 16 convolution layers was designed. In [24], a hybrid approach was presented which combined the criteria of CNN and genetic algorithm (GA) to enhance the network architecture.

In MR imaging classification, a key challenge lies in reducing the semantic gap between the high-level and low-level visual information obtained by tumor evaluator and MR imaging machine respectively. For this, a famous deep learning approach called convolutional neural networks (CNNs) can be used as a feature extractor to capture the relevant features for classification. Feature maps in the initial layers and higher layers of CNN extract low-level and high-level content (domain) specific features, respectively. Feature maps in the earlier layer construct simple structural information, for instance, shape, textures, and edges, whereas these low-level features are combined in higher layers to construct efficient model by integrating the global and local information.

3. System Model:

This section discusses about the proposed technique for detecting brain tumor by analysing the cell python `Objective_2\preprocess.py` of brain. The overall architecture has been given in figure-1.

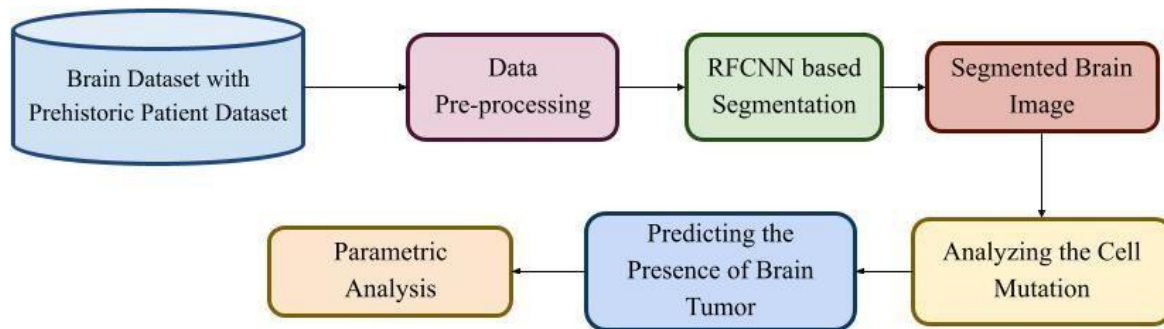


Figure-1 Proposed Architecture for brain tumor detection

From the above image, initially the dataset has been pre-processed for noise removal, filtering and image resizing. Then the pre-processed image has been segmented using proposed region based fast convolutional neural network. Then output of RFCNN will be segmented brain image and then the analysis for cell mutation is carried based on the confusion matrix of simulation output. By this the presence of brain tumor has been predicted and determined through parametric measures like accuracy, precision, recall, F-1 score, True positive and false positive rates.

3.1 Pre-processing of input training image:

Histogram pixel localization is used to enhance contrast. It is not necessary that contrast will always be increase in this. Then the noise of image has been removed using median filter which is integrated here. On basis of theory of probability, gray mapping for pixels has been recognized by Histogram pixel localization algorithm and gray functions as well as their transforms of the histogram has been parallel, even also they levelled up the gray scales, which leads to the function of enhancing the image has been attained. When the value of gray scale in input image pixel is $(0 \leq r \leq 1)$ then the probability of their intensity is $p(r)$, the value of gray scale for the image which is enhanced is $(0 \leq s \leq 1)$ then the probability of their intensity is $p(s)$, along with their operation of mapping is $s=T(r)$. According to the histogram physics, it is clear that every bar on the equalized histogram is of the equivalent height. That is shown by eq. (1)

$$p(s) = \sum_{r: T(r)=s} p(r) \quad (1)$$

When $s=T(r)$ is a operation that maximizes gradually with their time interval along with their operation of inverse as $r=T^{-1}(s)$ is a monotonic operation. Based on (1), (1) is assumed as in eq. (2),

$$p(s) = \sum_{r: T(r)=s} p(r) \quad (2)$$

The algorithm for normalization of conventional histogram: By the circumstances of discrete, the correlation among i (the value of gray scale in input image pixel) along with j (the value of gray scale for the image which is enhanced) is shown in eq. (3)

$$p(s) = \sum_{r: T(r)=s} p(r) \quad (3)$$

The number of levels in grayscale available in input image is given as m , the number of image pixel by their gray scale level of k th range is given by q_k , the image with average number of pixel is given by Q . when image is with various grayscale levels has been represented as n , then their rate of probability for i th gray scale level is p_i , then their level of grayscale of entropy has been given eq. (4)

$$H = - \sum_{i=1}^n p_i \log p_i \quad (4)$$

Entropy of entire image is given eq. (5)

$$H = - \sum_{i=1}^n p_i \log p_i \quad (5)$$

The entropy can be attained their maximum level only when $p_1 = p_2 = \dots = p_n = \frac{1}{n}$.

When the image has equal distribution of histogram has been attained through the maximum entropy of the image. The equation (3) shows the level of maximized dynamics of the image by this normalization. The property of normalization has been extended quantization interval.

3.2 Performance of median filter for noise reduction:

Since median filter is nonlinear filter, their arithmetic evaluation has been comparatively complicated by random noise of image. By normal distribution of zero mean image, the variance of noise for filtering by median filter is given eq. (6),

$$me d = \frac{1}{4nf^2(n')} \approx \frac{\sigma_i}{n+\frac{\pi}{2}-1} \frac{\pi}{2} \tag{6}$$

The variance of input power with noise is given by , the mask of median filter size is given as, the intensity of noise by their operation has been given as ('). The whole filtering of variance by noise is given eq. (7),

$$= \tag{7}$$

Equating equation 6 and 7, the impacts of median filter has been relies on two aspects, mask size and the noise distribution. The performance of filtering process of median for random noise has become optimized by minimizing than the simulation of typical filtering process, however for noise which is impulse, specifically contracted pulses has been apart as well as the breadth of pulses has been minimized by n/2, so the filtering process by median filter is highly efficient. The median filter has been enhanced when the median filtering is integrated with the average filtering where they can resize their mask in accordance with noise intensity.

3.3 Region based fast convolutional neural networks (RFCNN):

The training of RFCNN usually initiate (figure 2) with classification of image net with application of source along with their dataset, also network training done using supervision, along with the transform of network for the application of target with their dataset by fine-tuning of supervision. This technique has been correlated by general learning of multi-task but the sequential task has been trained along with extreme simulating by target task.

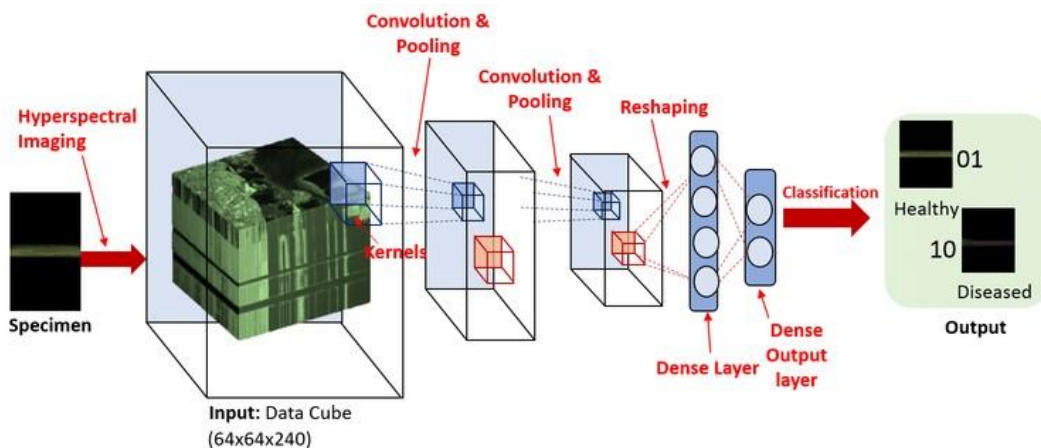


Figure 2- Proposed RFCNN architecture

Subsequently CNN has layer of fully connected cannot be handled by the indication frequency along with their varied objects. Thus the way to utilize sliding window brute force search in selecting the region along with the application CNN technique with that, here the problem is that this technique same for object depicts the image by various size and ratio of aspect. During the consideration of these parameters there exist maximum region for proposal also there the CNN is applied. The system of RFCNN functions by the algorithm of selective search which usually creates 2000 region for proposal. All the region proposal has been offered by CNN architecture which evaluates the feature of CNN. For classification these features are passes over the SVM model in which the object has been presented for region proposal. To execute the bounding box regressor, the object localization has been required by the image with higher accuracy.

In general RFCNN has 5 major stages:

1. The input image undergoes Selective search operation where they can select various proposed regions of maximum standard. Usually these proposed regions have been selected with various scales along with the various size and shape. Every proposed region has been labelled for category and ground-truth bounding box.
2. CNN is selected and placed for pre-training which has been minimized before the layer of output. Each proposed region has been transmitted to input dimensions needed through the network along with the evaluation uses for resulting features that are extracted by the proposed regions.
3. Each proposed region has been combined with features and class of labelling, where their example is for training the various SVM in classification of object. For determining each SVM particular classes are required.
4. Every proposed region has been combined with features along with box of bounding label where this has example in training model of linear regression for ground-truth bounding box prediction.
5. Even though pre-trained CNN models have been used by RFCNN for efficient feature extraction from the image, then the speed has been reduced by main downside. Since we use numerous proposed regions for single image, this requires the evaluation from CNN in detecting the tumor.

3.4 Loss Function

The loss function which is a multi-task loss is given as

$$L(\{p_i\}, \{t_i\}) = \frac{1}{N} \sum_i L_{reg}(p_i, t_i) + \frac{1}{N} \sum_i L_{cls}(p_i, t_i) \quad (8)$$

Here, p_i denotes the probability of predicted output, p_i^* represents ground truth, t_i indicates the predicted bounding box, t_i^* is the ground truth of the bounding box and is the classification loss while smooth loss is represented as L_{reg} .

The offset in regression is computed from the closest anchor box. Anchor boxes acts as region proposals in order to link this with region proposal approach. The feature map with 40×60 of size contains $40 \times 60 \times 9 \sim 20000$ anchor boxes in total. Every anchor box do not produce loss during training. When $IOU > 0.7$, anchors are assigned with positive labels and when $IOU < 0.3$, negative labels are assigned. Anchors labelled as neither positive nor negative, have no contribution towards then objective of training. Anchors with Crossboundaries are ignored.

3.5 RoI Pooling layer and Classifier layer

- The function RoI Pooling processes RoI producing an output with specific size using max pooling. Every ROI given as input is split as sub-cells to which max pooling is applied. Total sub-cells is the shape dimension of output. The last layer of the model is the classifier layer which is next to RoI Pooling layer. This is used for predicting class name for every anchor given as input and regression for bounding box.
- ROI pooling layer, a distinct case of spatial pyramid pooling (SPP) layer, has one level of pyramid. Features of selected proposal windows are divided into sub-windows with h/H by w/W as its size. Pooling operation is performed at every sub-window which produces fixed-size output features with $H \times W$ as its size which is not based on the size of the input. H and W are selected in such a way that output is compatible with FC layer in the network. Similar to that of regular pooling, ROI pooling is performed separately in each channel.
- ROI Pooling layer outputs the features which are fed to the FC layers softmax and BBregression branches. The former yields probability values for every ROI of K classes and one class of catch-all background. While the latter is involved in making precise bounding boxes from region proposal algorithm.

3.6 Performance analysis:

The experimental results of the proposed RFCNN for the brain cell mutation detection is discussed in this section. The commonly used openly available dataset from figshare is used to evaluate the algorithms. It comprises of 3064 MRI brain images of .mat format with size 512×512 which belong to the T1-CE MRI modality including coronal, sagittal and axial views. It contains 1426 MRI brain images with glioma, 708 images for meningioma and 930 images corresponding to pituitary tumor. GoogLeNet designed for RGB images has the input layer with size $224 \times 224 \times 3$.

3.7 Experimental setup

The entire implementation of the proposed RFCNN is carried out in Python and the system configuration is PC with Ubuntu, 4GB RAM, and Intel i3 processor.

3.8 Performance Metrics

The confusion matrix considered evaluation is based on the evaluation of other parameters like accuracy, precision, recall, and F1 - Score. The stated parameters are evaluated with the estimation of True Positive (TP), False Negative (FN), True Negative (TN), and False Positive (FP).

3.8.1 Accuracy: It defined the number of correctly predicted values to the total predictions. It is defined in equation (9)

$$\text{Accuracy} = \frac{TP + TN}{TP + TN + FP + FN} \quad (9)$$

TP, TN, FP, FN

3.8.2 Recall or Sensitivity: It is defined as the correctly predicted value to the total prediction value. It is defined in equation (10)

$$\text{Recall} = \frac{TP}{TP + FN} \quad (10)$$

3.8.3 Precision: It provides the ratio of true positive values to the total predicted values. It is stated in equation (11)

$$\text{Precision} = \frac{TP}{TP + FP} \quad (11)$$

TP, FP

3.8.4 F1 - Score: It provides the ratio between average mean of precision and recall. F1-Score is stated in equation (12)

$$F1\text{-Score} = 2 * \frac{\text{Precision} * \text{Recall}}{\text{Precision} + \text{Recall}} \quad (12)$$

3.8.5 Confusion Matrix: It provides the efficiency of the proposed model with a comparative analysis of actual and predicted values. The analysis is based on the estimation of TP, FN, FP, and TN. It is represented in equation (13)

$$\text{ConfusionMatrix} = \begin{bmatrix} TP & FP \\ FN & TN \end{bmatrix} \quad (13)$$

Where, True Positive (TP) is stated as forecast value which is anticipated as positive an AI model.

False Positive (FP) is defined as forecast value which is estimated as negative initially and later anticipated as positive in AI model.

True Negative (TN) demonstrated forecast value as negative and anticipated as unfavorable for AI model.

False Negative (FN) is stated as forecast value which is estimated as positive initially and later anticipated as negative in AI model.

Confusion matrix for cancer detection using proposed method is given by figure-3. Here the actual class and predicted class have been calculated with the confusion matrix based on normalization.

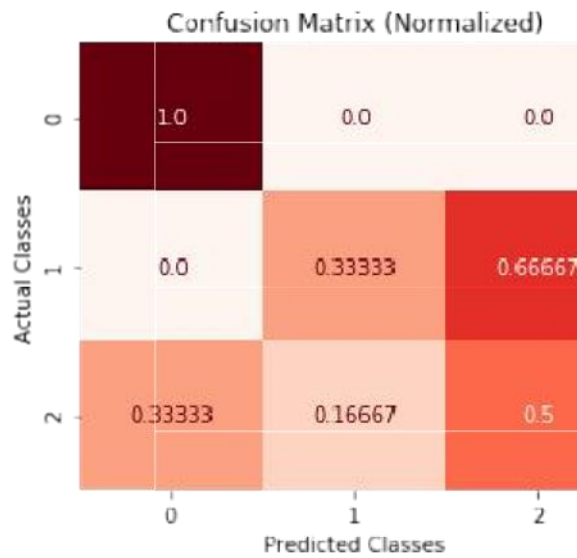


Figure-3 Confusion matrix

Table-1 shows overall parametric analysis comparatively between existing and proposed technique. The figures show comparative analysis graphically.

Table-1 Overall Performance

Parameters	CNN	KNN	SVM	RFCNN
Accuracy	88	89	91	93
Precision	86	85	84	87
Recall	77	75	76	79
F1-Score	79	80	81	82

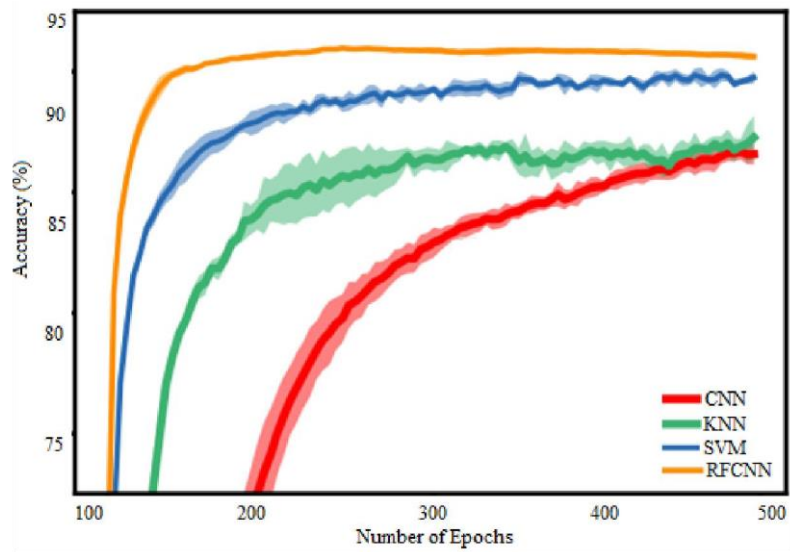


Figure -4 Comparison of Accuracy

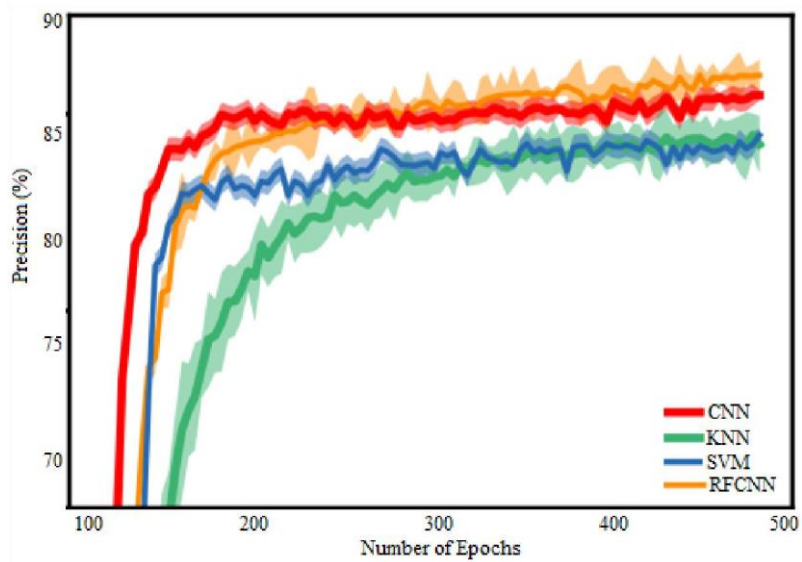


Figure-5 Comparison of Precision

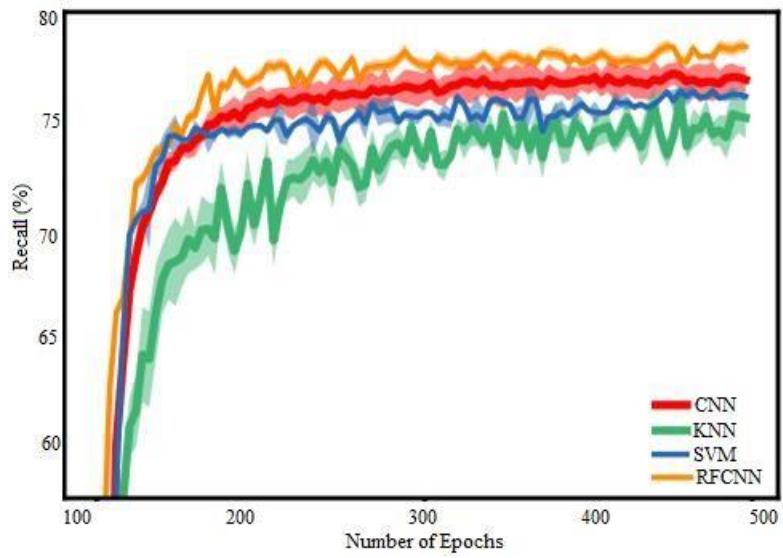


Figure-6 Comparison of Recall

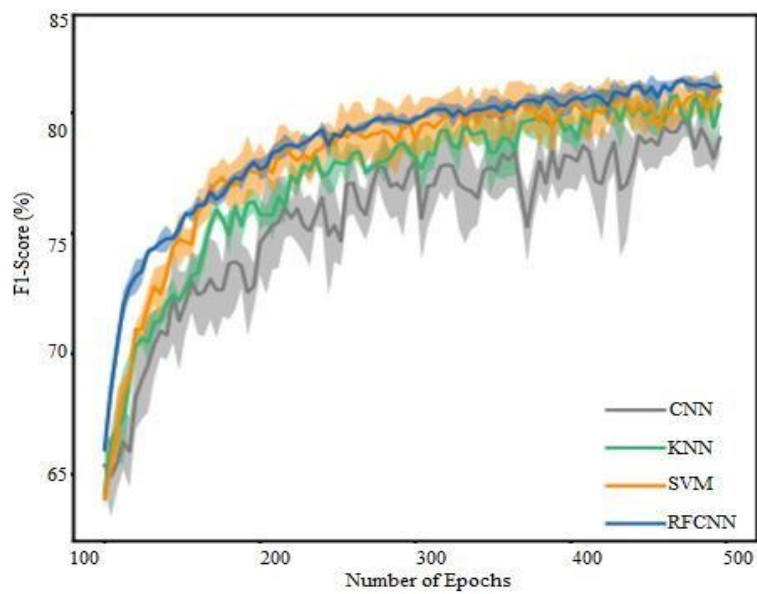


Figure-7 Comparison of F1- score

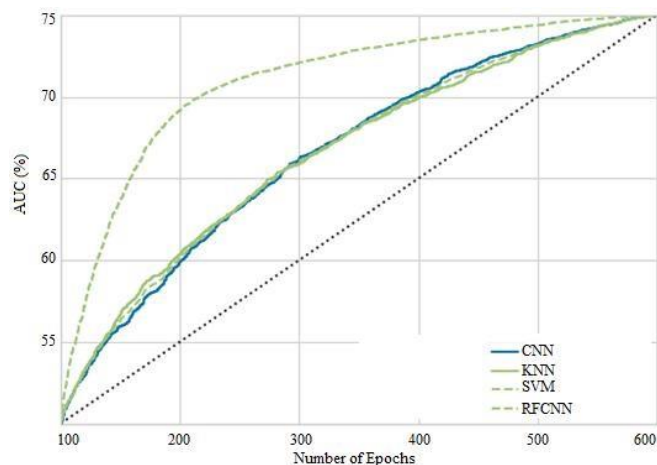


Figure-8 Comparative analysis of AUC

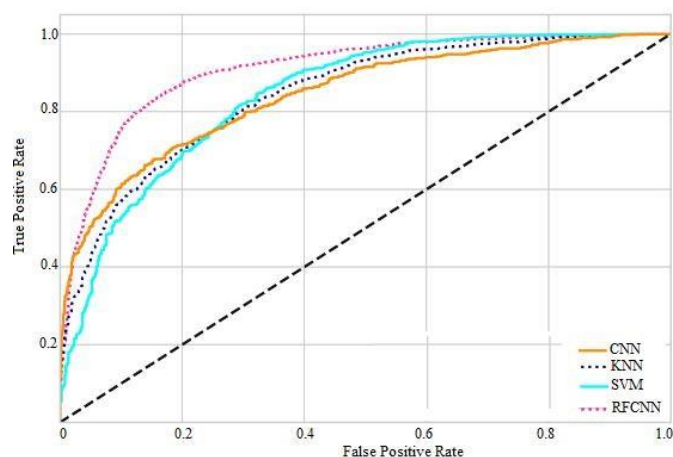


Figure-9 Comparison of TPR and FPR

The above figure 4-9 shows the performance of proposed model of brain tumor cell mutation. The performance of this model is estimated with fivefold cross-validation for classification. The 4 sets of data are used for training while the other for testing. Here the parameters analysed are accuracy, precision, recall, F1- score, AUC, TPR and FPR. By this analysis it is evident that the proposed technique shows enhanced output for tumor detection. The RFCNN obtained accuracy of 93 %, precision of 87%, recall of 79% and F1- score of 82%. The plot for accuracy, precision, recall and F-1 score has been taken with each parameter versus epochs. Classification of datasets has been achieved by these parameters using the proposed model after 294 iterations which shows the effectiveness of the proposed model for the classification of brain tumor.

Conclusion:

Brain tumor is formed due to the abnormal cells of brain or central spine canal which can either be cancerous or noncancerous. The former is termed as malignant while the latter is benign. When a growth is found on the tumor, there is an increase in the pressure on skull. Further, brain tumors are classified as primary or secondary. The former originates from brain while most of them are benign. The latter, also termed as metastatic brain tumor, is experienced due to the spreading of the cancer cells to brain from other parts of the body. Death rate can be reduced by saving lives when tumors are detect at the early stage. Brain tumor detection undergoes several complex stages and is also time consuming. This paper proposed segmentation technique in detecting tumor using RFCNN. Here the segmented data is used for analysing the cell mutation in detecting whether it is cancerous cell or non-cancerous cell. By this analysis the primary and secondary type of brain tumor has been segmented. Once the segmentation is carried out, the prediction for presence of tumor has been done by obtaining the confusion matrix. The actual and predicted class shows the presence of cancerous cell or non-cancerous cell. Finally, by experimental results, the accuracy obtained is 93%, precision of 87%, recall of 79% and F1-

score of 82%. When compared with existing techniques, the proposed technique obtains enhanced results in detecting tumor. In future, this method can be enhanced for categorical classification like identifying the types of brain tumor or can be involved in detecting the other abnormalities in brain. Moreover, this developed system is expected to be effective for early diagnosis of disease in other domains like lung or breast cancer as their death rate is high across the world. This model can even be used in other scientific fields where larger dataset is not available or other transfer learning approaches can be used with this proposed model.

Reference:

1. Md. Rezwanul Islam, Md. Rizwan Imtiaz, Marium-E-Jannat, Detection and analysis of brain tumor from MRI by Integrated Thresholding and Morphological Process with Histogram based method, IEEE 2018
2. Harshini Badisa, Madhavi Polireddy, Aslam Mohammed, CNN Based Brain Tumor Detection, ISSN: 2249 – 8958, 8 (4), April 2019
3. Bashayer Fouad Marghalani, Muhammad Arif, Automatic Classification of Brain Tumor and Alzheimer's Disease in MRI, 2019
4. J. Seetha and S. Selvakumar Raja, Brain Tumor Classification Using Convolutional
5. Neural Networks, 11(3), p. 1457-1461, 2018
6. Rachapudi, V., Lavanya Devi, G. Improved convolutional neural network based histopathological image classification. Evol. Intel. (2020). <https://doi.org/10.1007/s12065-02000367-y>
7. Krishnaraj, V., Jaisharma, K., & Deepa, N. (2019). Real time brain tumor detection using deep reinforcement learning algorithm. Test Engineering and Management, 81(11-12), 5370-5379. Retrieved from www.scopus.com.
8. Kurade, M., Nakil, N., Pai, S., Ringane, V., & Akulwar, P. K. A Survey on Brain Tumor Detection using Machine Learning.
9. Kang, J., Ullah, Z., & Gwak, J. (2021). MRI-Based Brain Tumor Classification Using Ensemble of Deep Features and Machine Learning Classifiers. Sensors, 21(6), 2222.
10. Sharif, M. I., Li, J. P., Naz, J., & Rashid, I. (2020). A comprehensive review on multiorgans tumor detection based on machine learning. Pattern Recognition Letters, 131, 30-37.
11. Amin, J., Sharif, M., Raza, M., & Yasmin, M. (2018). Detection of brain tumor based on features fusion and machine learning. Journal of Ambient Intelligence and Humanized Computing, 1-17.
12. Tarik, H., Tawfik, M., Youssef, D., Simohammed, S., Mohammed, O. J., & El Miloud, J. (2019, November). Towards an improved CNN architecture for brain tumor classification. In International Conference Europe Middle East & North Africa Information Systems and Technologies to Support Learning (pp. 224-234). Springer, Cham.
13. Garg, S., & Bhagyashree, S. R. (2019, February). Detection and Classification of Tumors Using Medical Imaging Techniques: A Survey. In Intelligent Communication Technologies and Virtual Mobile Networks (pp. 363-372). Springer, Cham.
14. Havaei, M.; Davy, A.; Warde-Farley, D.; Biard, A.; Courville, A.; Bengio, Y.; Pal, C.; Jodoin, P.-M.; Larochelle, H. Brain tumor segmentation with deep neural networks. Med. Image Anal. 2017, 35, 18–31.
15. Havaei, M.; Jodoin, P.-M.; Larochelle, H. Efficient Interactive Brain Tumor Segmentation as Within-Brain kNN Classification. In Proceedings of the 22nd International Conference on Pattern Recognition, Stockholm, Sweden, 24–28 August 2014; IEEE: Los Alamitos, CA, USA, 2014; pp. 556–561.
16. Moeskops, P.; de Bresser, J.; Kuijff, H.J.; Mendrik, A.M.; Biessels, G.J.; Pluim,
17. J.P.W.; Išgum, I. Evaluation of a deep learning approach for the segmentation of brain tissues and white matter hyperintensities of presumed vascular origin in MRI. NeuroImage Clin. 2018, 17, 251–262.

18. MRBrainS: Evaluation Framework for MR Brain Image Segmentation. Available online: <https://mrbrains13.isi.uu.nl/> (accessed on 12 December 2020).
19. Ronneberger, O.; Fischer, P.; Brox, T. U-Net: Convolutional Networks for Biomedical Image Segmentation. In Proceedings of the 18th International Conference on Medical Image Computing and Computer-Assisted Intervention—MICCAI, Munich, Germany, 5–9 October 2015; Navab, N., Hornegger, J., Wells, W., Frangi, A., Eds.; LNCS. Springer: Cham, Switzerland, 2015; Volume 9351, pp. 234–241.
20. ISBI Challenge: Segmentation of Neuronal Structures in EM Stacks. Available online: http://brainiac2.mit.edu/isbi_challenge (accessed on 15 December 2020).
21. Mohsen, H.; El-Dahshan, E.-S.A.; El-Horbaty, E.-S.M.; Salem, A.-B.M. Classification using deep learning neural networks for brain tumors. *Future Comput. Inform. J.* 2018, 3, 68–71. [CrossRef]
22. Abiwinanda, N.; Hanif, M.; Hesaputra, S.T.; Handayani, A.; Mengko, T.R. Brain tumor classification using convolutional neural network. In Proceedings of the World Congress on Medical Physics and Biomedical Engineering, Prague, Czech Republic, 3–8 June 2018; Springer: Singapore, 2019; pp. 183–189.
23. Kumar, S. (2022). A quest for sustainium (sustainability Premium): review of sustainable bonds. *Academy of Accounting and Financial Studies Journal*, Vol. 26, no.2, pp. 1-18
24. Allugunti V.R (2022). A machine learning model for skin disease classification using
25. convolution neural network. *International Journal of Computing, Programming and Database Management* 3(1), 141-147
26. Pashaei, A.; Sajedi, H.; Jazayeri, N. Brain Tumor Classification via Convolutional Neural Network and Extreme Learning Machines. In Proceedings of the 8th International Conference on Computer and Knowledge Engineering (ICCKE), Mashhad, Iran, 25–26 October 2018; Curran Associates: New York, NY, USA, 2018; pp. 314–319. 4
27. Sultan, H.H.; Salem, N.M.; Al-Atabany, W. Multi-classification of brain tumor images using deep neural network. *IEEE Access* 2019, 7, 69215–69225. [CrossRef]
28. Anaraki, A.K.; Ayati, M.; Kazemi, F. Magnetic resonance imaging-based brain tumor grades classification and grading via convolutional neural networks and genetic algorithms. *Biocybern. Biomed. Eng.* 2019, 39, 63–74.
29. Mazurowski, M.A.; Buda, M.; Saha, A.; Bashir, M.R. Deep learning in radiology: An overview of the concepts and a survey of the state of the art with focus on MRI. *J. Magn. Reson. Imaging* 2019, 49, 939–954